nanomanufacturing

MDPI

Article

Carbonization of Biopolymers as a Method for Producing a Photosensitizing Additive for Energy Materials

Mikhail Alekseevich Ilyushin [1,*], Alexander Petrovich Voznyakovskii [1,2], Irina Shugalei [1] and Aleksei Alexandrovich Vozniakovskii [3]

[1] Department of Chemistry and Technology of Organic Nitrogen Compounds, St. Petersburg State Institute of Technology, 190013 Saint Petersburg, Russia; voznap@mail.ru (A.P.V.); shugalei@mail.ru (I.S.)
[2] Lebedev Research Institute for Synthetic Rubber, 198035 Saint Petersburg, Russia
[3] Ioffe Institute, 194021 Saint Petersburg, Russia; alexey_inform@mail.ru
* Correspondence: explaser1945@gmail.com or explaser1945@yandex.ru

Abstract: It has been shown that defect-free Stone–Wales (SW) free few-layer graphene (FLG) can be obtained by carbonizing lignin under conditions of self-propagating high-temperature synthesis (SHS). The obtained few-layer graphene was used as a modifying additive for pyrotechnic compositions. It was found that the addition of 2.5 mass % of few-layer graphene synthesized from lignin to a pyrotechnic complex based on porous silicon and fluoropolymer leads to a significant increase in the combustion intensity of pyrotechnic compositions.

Keywords: few-layer graphene; nanoporous silicon; pyrotechnic composition; laser radiation; fluoroelastomer

check for updates

Citation: Ilyushin, M.A.; Voznyakovskii, A.P.; Shugalei, I.; Vozniakovskii, A.A. Carbonization of Biopolymers as a Method for Producing a Photosensitizing Additive for Energy Materials. *Nanomanufacturing* **2023**, *3*, 167–176. https://doi.org/10.3390/nanomanufacturing3020011

Academic Editors: Alexander Pyatenko and Alejandro Rodriguez Pascual

Received: 30 March 2023
Revised: 26 April 2023
Accepted: 3 May 2023
Published: 9 May 2023

Copyright: © 2023 by the authors. Licensee MDPI, Basel, Switzerland. This article is an open access article distributed under the terms and conditions of the Creative Commons Attribution (CC BY) license (https://creativecommons.org/licenses/by/4.0/).

1. Introduction

According to data from the International Lignin Institute (ILI, Lausanne, Switzerland), using wood as a raw material for biochemical production leads to the generation of much industrial waste, technical lignin, in amounts of millions of tons. Even though lignin (the second most abundant natural polymer on earth) is extensively used in both the original and modified forms [1–3], large-capacity processing and the utilization of technical lignins remain problematic.

The main difficulty of processing large amounts of lignin lies in the high-energy intensity of the techniques and the high costs of reagents used to modify technical lignins. Therefore, the current research activities in the field of utilization of wood-processing industry waste are focused on the search for new, cheaper, and less energy-intensive, lignin processing methods, as well as for new applications of this material in both the original and modified forms [4]. These methods will serve a dual purpose of utilizing lignin as an industrial waste and of taking maximum advantage of the potential offered by technical lignin for application as a raw material in new chemical technologies. Despite considerable efforts undertaken by many research teams during a prolonged (nearly a century-long) period, the problem of elimination of hydrolysis lignin waste dumps is still a long way from being solved. In a review [5], the authors noted that the main reason for this is the complex composition of lignin, the complexity of its processing, and the high equipment cost. As a result, lignin-based products are too expensive and cannot compete with already known materials. Therefore, researchers seek new ways to process lignin into a high-added-value product [6]. However, classical chemical and biochemical approaches have limited applicability to lignin processing because of its unique structure. We have recently shown that lignin can be efficiently and cost-effectively recycled by carbonizing it under the self-spreading high-temperature synthesis process [7].

The purpose of this work was to demonstrate the possibility of transforming lignin into high-quality GNS, namely few-layer graphene (FLG with no more than 10 layers [8])

suitable for use as a modifying additive in the creation of pyrotechnic compositions based on promising fuel-porous silicon [9]. The addition of FLG increases the sensitivity of pyrotechnic compositions to laser radiation based on porous silicon (por-Si). Porous silicon as a fuel was chosen based on the results of publication [10], which showed that the charges of the pyrotechnic composition (por-Si + $Ca(ClO_4)_2$) were insensitive to laser radiation from a laser diode with a constant flux q ≈ 15 mW/m^2 (wavelength 450 nm, laser beam diameter d = 2 mm). However, after adding few-layer graphene FLG (20–30 mass %) to the pyrotechnic composition, laser initiation led to the ignition of charges with a strong sound effect, which could be classified as a deflagration mode. Thus, these results motivated us to use porous silicon as fuel in our work.

Modern stringent requirements for the reliability and safety of the initiation of pyrotechnic compositions lead to research groups moving from initiation by dynamic shock loads to initiation by laser radiation [11]. Successful experiments on laser ignition of pyro compositions based on fluoropolymers are known [12]; moreover, tetrafluoroethylene-based pyrotechnics are capable of both burning and detonating [13]. In the presented work, copolymer of vinylidene fluoride with trifluorochloroethylene (SKF-32) was used as a fluoroxidant in pyrotechnic compositions, which has a technological advantage over fluoropolymers previously used in pyrotechnic compositions. Selected fluoroelastomer is highly soluble in acetone, which makes it possible to simplify and secure the process of preparing pyrotechnic compositions by replacing the mechanical mixing of fuel and oxidizer powders with the ultrasonic mixing of fuel powders in a solution of a fluoroelastomer in acetone.

2. Experimental Part

2.1. Materials and preparation

2.1.1. Materials

As a source material for the synthesis of few-layer graphene (FLG) lignin was taken. Lignin was obtained from the waste of the long-term storage of the Arkhangelsk Pulp and Paper Mill. Arkhangelsk Pulp and Paper Mill's lignin was preliminarily dried to a constant weight in a drying cabinet ShS-40-02 at 80 °C. The dried lignin powder was finally crushed in a laboratory planetary mill LP-1-HT Machinery (Japan) and sifted through a sieve to a particle sizes of about 100 μm (±10 μm).

2.1.2. Initial Pyrotechnic Compositions

Porous silicon (KDB-100, Russian Federation) with a porosity of ~80% was used as the starting material for the synthesis of the pyrotechnic composition. Fluoroelastomer (vinylidene fluoride copolymer with trifluoroethylene (SKF-32, GOST 18376-79)) was used as a model fluoroxidizer for porous silicon. The structural formula of fluoroelastomer is given below:

$$[(\text{-}CF_2\text{-}CFCl\text{-})_m(\text{-}CH_2\text{-}CF_2\text{-})_p]_n$$

Fluoroelastomer SKF-32; *m*, *p*, *n*–coefficients.

Ammonium nitrate (NH_4N0_3, chemically pure, Sigma-Aldrich, St. Louis, MO, USA).

2.2. Methods

2.2.1. Synthesis of Few-Layer Graphene (FLG)

Synthesis of few-layer graphene (FLG) was carried out under the conditions of a self-sustaining high-temperature synthesis process (SHS). To obtain FLG, lignin powder was mixed with an oxidizing agent (ammonium nitrate) in a ratio of 1:1, and the resulting mixture was placed in the reactor and heated to a temperature of 220 °C using an oil bath. The detailed synthesis procedure is described in [14]. The model of 2D nanocarbon formations in the SHS process is shown in Figure 1. Under the combination of extremely high temperatures and an aggressive gaseous environment, lignin degrades to asphaltene primitives, which organize into graphene structures.

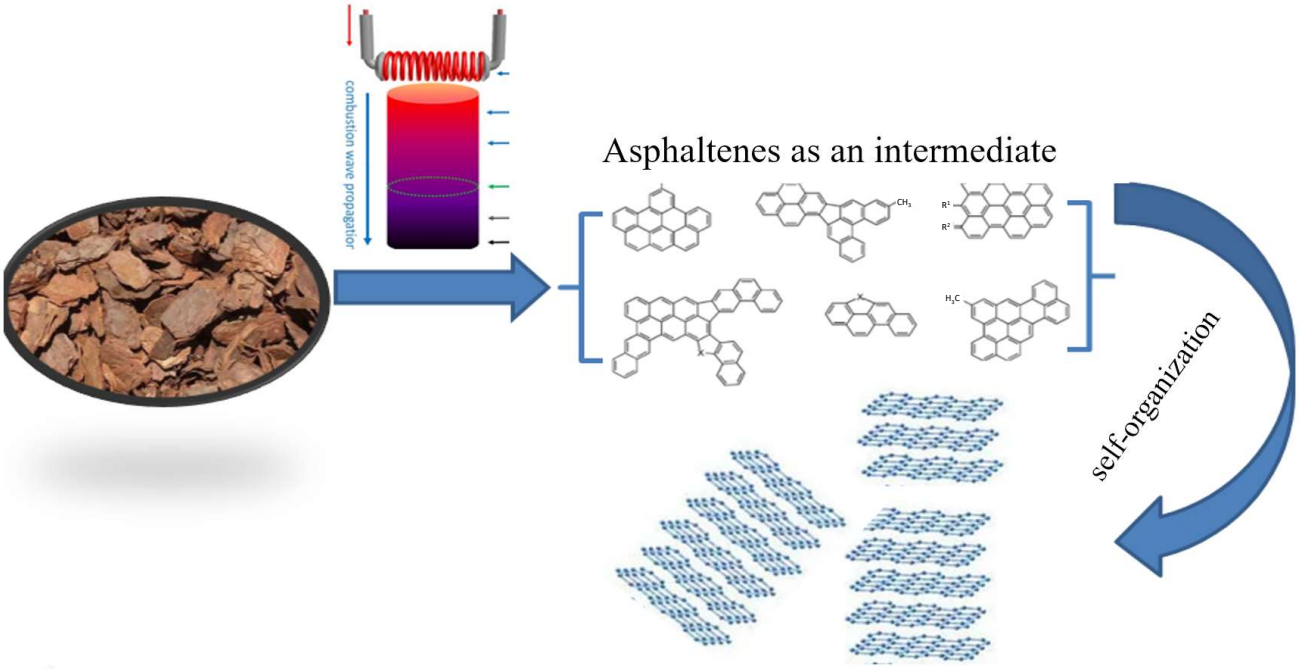

Figure 1. Schematic representation of lignin carbonization.

The product yield was 44 mass % (based on the initial amount of lignin).

2.2.2. Electron Microscopy

Electronic images of the few-layer graphene (FLG) sample were obtained using a TESCAN Mira-3M scanning electron microscope (SEM) (operated at 20 kV) and a FEI Tecnai G2 30 S-TWIN transmission electron microscope (operated at 50 kV). For transmission electron microscopy (TEM) analysis, a suspension of the FLG sample in toluene (concentration 0.05 mass %) was prepared, applied to a carbon grid and dried in a drying cabinet at 60 °C.

2.2.3. Dispersion Measurement

The laser diffraction method with a Mastersizer 2000 device, USA was used to study the dispersion of the synthesized material. A suspension of FLG particles in water (0.05 mass %) was prepared by sonication, an ultrasonic bath «Sapphire» (50 W, 22 kHz), for measurement purposes.

2.2.4. X-ray Diffraction

X-ray phase analysis was carried out using a Shimadzu XRD-7000 diffractometer (Cu Kα = 0.154051 nm). The scanning rate was 1 deg/min.

2.2.5. Raman Spectroscopy

Raman spectroscopy was carried out on a Confotec NR500 instrument (532 nm, SOL Instruments, Minsk, Belarus). For measurement purposes, a suspension of the FLG sample in toluene (concentration of 0.05 mass %) was prepared, applied onto a silicon plate, and dried in a drying cabinet at 60 °C.

2.2.6. Specific Surface Area Measurement

The specific surface area of the FLG sample was measured using ASAP 2020 instrument, USA, by the Brunauer–Emmett–Teller (BET) method. Before measurement, the FLG sample was dried for 2 h at 300 °C under vacuum.

2.2.7. Determination of Stone–Wales Defect Concentration (S-W)

To quantitatively determine the concentration of S-W defects in the synthesized sample, the original method based on the 2,4-diene synthesis reaction was used [15]. A mixture of α-methylstyrene and o-xylene in equal proportions was added to the suspension of few-layer graphene in toluene. α-methylstyrene was chosen as a conjugated diene because, unlike classical dienes, such as cyclopentadiene and styrene, it is not subject to homopolymerization. The progress of the reaction was monitored by the controlled gas chromatography method of α-methylstyrene decrease in the reaction mixture. O-xylene was used as a standard (gas chromatograph Clarus 500, manufactured by Perkin-Elmer). The investigation parameters are as follows: column temperature—145 °C; detector temperature—250 °C; evaporator temperature—250 °C; gas rate—30 mL/min. Commercial single-walled carbon nanotubes (SWCNT) (OSiAl, RF) were used as a reference sample.

2.2.8. Synthesis of the Pyrotechnic Composition

The starting porous silicon (por-Si) powder was mixed with FLG powder in a 'drunken barrel' type homogenizer for 30 min to obtain a homogeneous mixture. The FLG concentration was 1.25, 2.5, 5, and 10 mass %. The obtained mixtures were added to a 5% acetone solution of fluoroelastomer SKF-32 (fluorine content 54–56%) and mixed in an ultrasonic field (ultrasonic bath 'Sapphire', 50 W, 22 kHz) for 30 min at room temperature. As a result, samples of energy-saturated composite por-Si/FLG/SKF-32 were obtained with the following ratios: 50/1/25/48.75, 50/2.5/47.5, 50/5/45, and 50/10/40. A pyrotechnic composition with a 50/0/50 ratio of components was used as a reference sample. The introduction of a composite filler into the polymer solution volume led to the formation of a high-viscosity system, which can be attributed to the effective immobilization of polymer macrochains on the surface of composite filler particles. To eliminate the porosity of the obtained energy composite, it was dried in air at room temperature for 24 h in the first stage. Finally, the solvent was removed by holding it in an air thermostat for three hours at a temperature of 70–85 °C and for three hours at a temperature of 120–135 °C. The dried composition was a thin brown film (Figure 2).

Figure 2. Appearance of the composition por-Si/FLG/SKF-32.

2.2.9. Investigation of Pyrotechnic Compositions

To investigate the effect of FLG addition on the properties of pyrotechnic composition, the obtained por-Si/FLG/SKF-32 mixtures were irradiated with a laser diode beam (power 1 W, wavelength 450 nm, and pulse time ~10 ms). The process of films burning from pyrotechnic compositions during laser ignition was recorded by the main camera of the Honor 10 smartphone (16 MP, aperture f/1.8), frame rate 720 fps (or 480 fps).

3. Results and Discussion

Figure 3 shows the electronic images of the synthesized FLG sample obtained by scanning electron microscope (SEM) and transmission electron microscope (TEM) methods.

As seen in Figure 3, the synthesized particles have a few-layer structure and linear dimensions of up to several tens of microns, which is confirmed by the results of the particle size distribution analysis using the laser diffraction method (Figure 4).

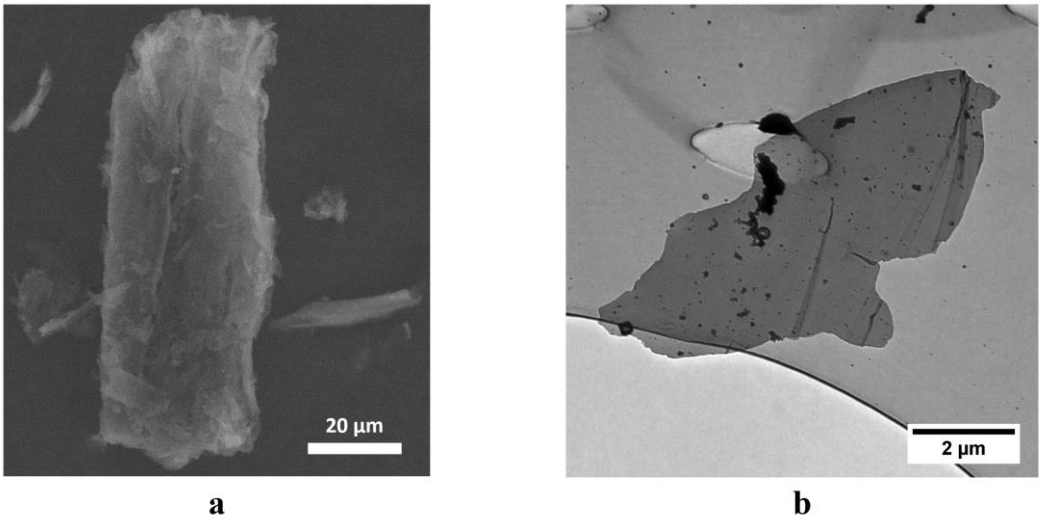

Figure 3. SEM and TEM images of FLG nanoplates synthesized from lignin. (**a**) SEM image, linear scale 20 µm, (**b**) TEM image, linear scale 2 µm.

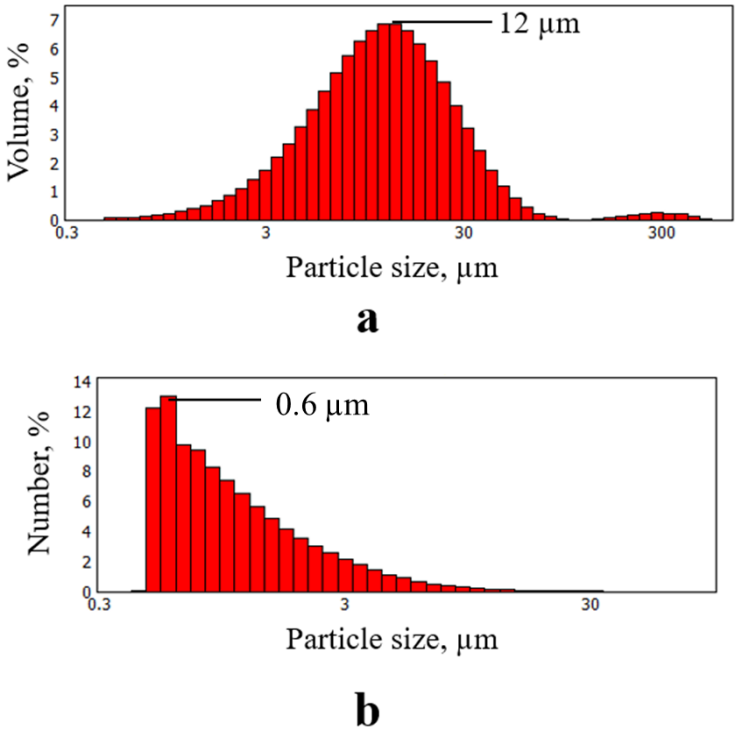

Figure 4. Results of FLG particles size distribution measurements. (**a**) Particle size distribution by volume; (**b**) Distribution of particle size by particle count.

To determine the number of layers in the synthesized FLG sample, an X-ray diffraction study was carried out, and the results are shown in Figure 5.

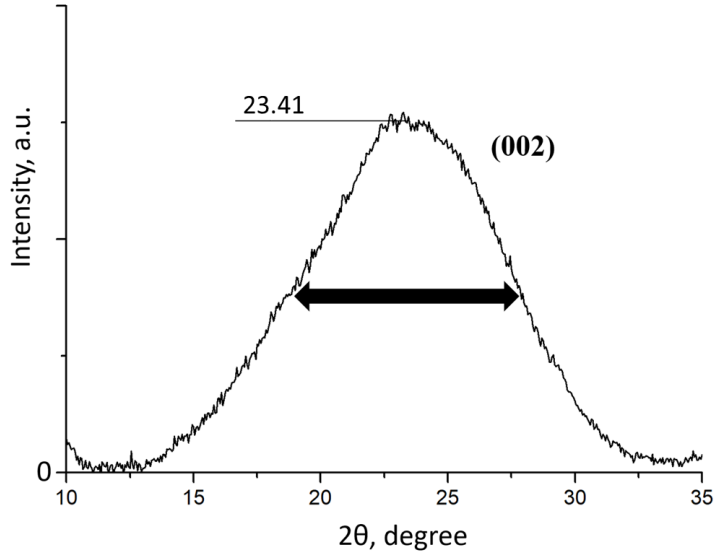

Figure 5. X-ray diffraction pattern of the FLG sample.

Based on the position of the 002 peak and its FWHM, the size of the crystal (L) was calculated using the Scherer formula [16], which was found to be 14.9 Å. The number of graphene layers in the sample was then calculated using the formula N = L/d, where N is the number of graphene layers in the sample and d = 3.65 A is the interplanar distance. As a result of the calculation, it was found that the number of graphene layers in the sample does not exceed five.

Figure 6 shows the Raman spectrum of the synthesized FLG sample. As it can be seen in Figure 6, the synthesized sample demonstrates a typical Raman spectrum for graphene nanostructures.

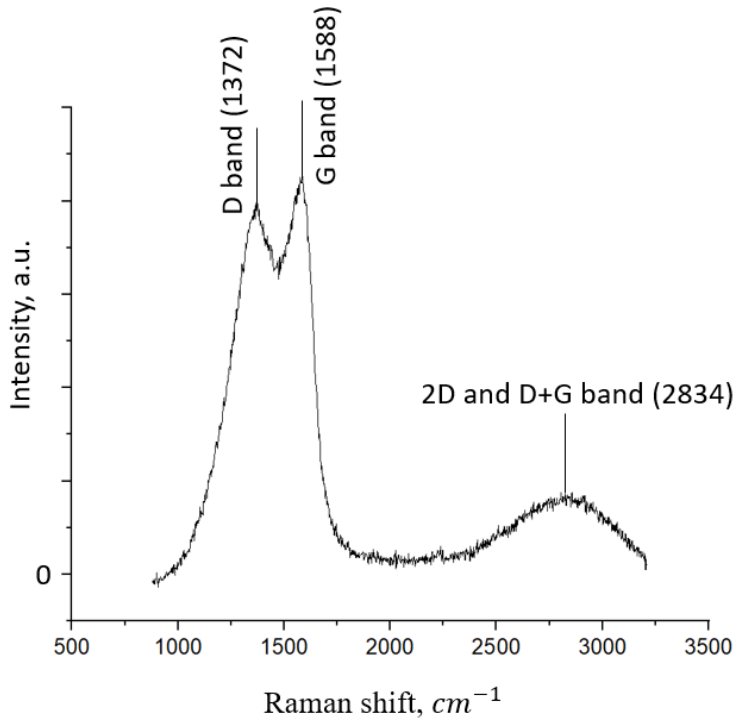

Figure 6. Raman spectrum of the FLG sample.

The intensity ratio of the D and G peaks is 0.96, which is similar to the Raman spectra observed in [17]. In [18], the authors linked the mutual overlap of the 2D and D + G peaks

in the 2500–3500 cm^{-1} region with the wavy structure of the samples, the presence of many edges, and the different directions of graphene layers overlapping.

The results of evaluating the defectiveness of the synthesized sample of few-layer graphene are presented in Table 1.

Table 1. Specific concentration of Stone–Wales defects in FLG.

Nanocarbon	Specific Surface Area, m^2/g	Stone–Wales Defects, $C_{SW} \times 10^5$ (mol/m^2)
SWCNT	300	1.1
FLG	320	0

As seen in Table 1, unlike the reference sample (SWCNT), the FLG sample does not contain S-W defects within the instrument's sensitivity.

Figure 7 shows the maximum geometric dimensions of the flame of burning por-Si/SKF-32 and por-Si/FLG/SKF-32 films, which served as a criterion for the intensity of the flame in the process of combustion of pyrotechnic compositions in this work. The duration of burning of pyrotechnic compositions after their laser ignition was an additional comparative criterion.

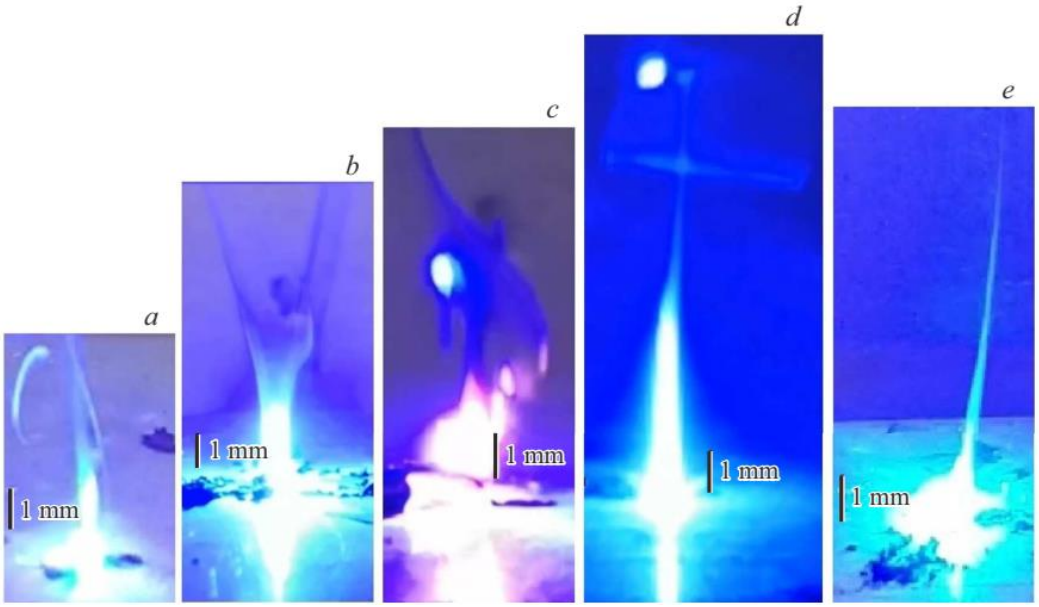

Figure 7. Maximum flame intensity of films. (**a**) Reference composition without FLG; (**b**) Composition with 1.25 mass % FLG; (**c**) Composition with 2.5 mass % FLG; (**d**) Composition with 5 mass % FLG; (**e**) Composition with 10 mass % FLG.

It was shown that the composition that does not contain FLG ignites under laser irradiation (Figure 7a); however, the burning process of the composition immediately stopped after the irradiation was completed. The obtained result can be explained as follows: under the influence of coherent radiation, fluoroelastomer SKF-32 undergoes destruction, releasing fluorine oxidizers into the gas phase. At the ignition temperature of the pyrotechnic composition, laser diode radiation oxidizes porous silicon to SiF_4 with HF according to the equation

$$Si\ (solid) + 4HF\ (g) \rightarrow SiF_4\ (g) + 2H_2SiF_4$$

SiF_4 is also formed upon the influence of gaseous CF_2 on porous silicon:

$$2CF_2\ (g) + Si\ (solid) \rightarrow SiF_4\ (g) + 2\ C$$

As a result of the ongoing redox reactions, the flame temperature is obviously below the optimum and ranges, apparently, from 200 °C to 320 °C (Figure 7a); therefore, only a portion of the fluoroelastomer undergoes degradation and depolymerization. Obviously, the entire amount of CF_2 and HF produced by laser radiation during the laser pulse interacts with the porous silicon, and the burning of the composite stops after the laser is turned off.

The laser diode initiation of por-Si/FLG/SKF-32 energy-composite films in the entire studied range of graphene content led to the excitation of the pyro-compositions combustion processes. Adding 1.25 mass % FLG to the por-Si/SKF-32 composition increased its burning intensity compared to the pure por-Si/SKF-32 mixture (see Figure 7a,b). Obviously, the phenomenon of photo-sensitization of polymer destruction by graphene served as the reason for the increase in the intensity of burning of the sample. It is known that under the influence of external factors, such as thermal heating or electric field, graphene nanostructures can serve as a source of electrons, allowing them to be used as emitter materials [19,20]. However, as shown in [21], the presence of S–W defects in graphene nanostructures significantly decreases their electrical and thermal properties. Previously, we have shown that FLG synthesized under SHS conditions from starch can be used as a cathode material for obtaining low-threshold field emission [22]. Based on the absence of S-W defects in FLG (see Table 1), it can be assumed that FLG can serve as a source of electrons. Consequently, due to the transfer of an additional electron to the SKF-32 macromolecule, it loses its thermal stability, more easily undergoes destruction, and more HF and CF_2 are formed. The critical stage of these processes is the transfer of charge generated by an external radiation source from the photocatalyst to the SKF-32 macromolecule, leading to the formation of a metastable anion radical capable of decomposing and initiating the process of accelerated polymer degradation.

It is also possible that the mechanism por-Si particle activation by FLG particles occurs during the oxidation processes of the pyrotechnic compositions. This assumption is based on the fact that porous silicon has areas with increased surface energy, with which FLG, probably due to sorption processes (physical or chemical), forms, which is associated with photocatalytic activity [23,24].

The burning intensity of films with FLG content of 2.5 mass % and mass 5% was higher than that of previously studied films Figure 7a,b (Figure 7c,d). It should be noted that only these two films of energy composites continued to burn after the end of exposure to the laser beam. For example, Figure 8 shows a photo of the combustion of a composition containing 2.5 mass % FLG 5 ms after laser irradiation.

Figure 8. Burn intensity of a film with 2.5 mass % FLG 5 after the laser beam was turned off.

Thus, in these compositions, the processes of SKF-32 polymer destruction and the formation of gaseous fluorinating agents proceed so intensively during laser irradiation; some amount of HF and CF_2 remains after the laser exposure is terminated, and the burning process of porous silicon continues for some time until the fluorinating agents are completely consumed. Based on Figure 7, the optimal catalytic effect of FLG in the studied pyrotechnic composition (as a photosensitizer) was observed with its 5 mass % introduction into the system due to the SKF-32 polymer. A further increase in the amount of graphene

in the composite to 10 mass % led to a decrease in the flame intensity and combustion time of the composition compared to those obtained in experiments Figure 7c,d (Figure 7e).

Consequently, the optimal catalytic effect of FLG as a photosensitizer in the studied pyrotechnic composition was observed when it was introduced in an amount of 5 mass % into the system at the expense of the SKF-32 polymer (Figure 7).

4. Conclusions

It was found that lignin can serve as a cheap and practically inexhaustible source of raw materials for synthesizing large volumes of few-layer graphene (FLG) under the conditions of the SHS process. It was experimentally shown that due to the absence of Stone–Wales defects in the synthesized few-layer graphene, it can be used as an effective additive in creating model pyrotechnic compositions of porous silicon/SKF-32 polymer with laser irradiation. The additive is already 2.5 mass % FLG, which made it possible to significantly increase the intensity of combustion of the pyrotechnic composition, which continued even after the cessation of laser irradiation. A possible mechanism for the influence of FLG on the properties of pyrotechnic compositions based on the decrease in thermal stability was proposed.

The article has only scientific value and the obtained results cannot be used in practice.

Author Contributions: Conceptualization, A.P.V. and M.A.I.; methodology, A.P.V., A.A.V. and M.A.I.; validation, I.S.; investigation, A.P.V. and A.A.V.; resources, A.P.V. and A.A.V.; data curation, A.P.V.; writing—original draft preparation, A.A.V., A.P.V. and M.A.I.; writing—review and editing, A.A.V., A.P.V., I.S. and M.A.I.; visualization, A.A.V.; supervision, M.A.I.; project administration, M.A.I.; funding acquisition, A.A.V. and M.A.I. All authors have read and agreed to the published version of the manuscript.

Funding: The work of Ilyushin M.A. supported by the RFBR grant 17-03-00566. The work of Vozniakovskii A.A. was supported by RFBR and BRFBR, project number 20-53-04026.

Data Availability Statement: Not applicable.

Conflicts of Interest: The authors declare that there are no conflicts of interest requiring disclosure in this article.

References

1. Krutov, S.M.; Voznyakovskii, A.P.; Gribkov, I.V.; Shugalei, I.V. Lignin Wastes: Past, Present, and Future. *Russ. J. Gen. Chem.* **2014**, *84*, 2632–2642. [CrossRef]
2. Fu, F.; Yang, D.; Zhang, W.; Wang, H.; Qiu, X. Green self-assembly synthesis of porous lignin-derived carbon quasi-nanosheets for high-performance supercapacitors. *Chem. Eng. J.* **2020**, *392*, 123721. [CrossRef]
3. Wang, H.; Feng, P.; Huang, P.; Huang, M.; Lin, X.; Feng, Y.; Gan, S.; Han, D.; Wang, W.; Niu, L. Solvent-induced molecular structure engineering of lignin for hierarchically porous carbon: Mechanisms and supercapacitive properties. *Ind. Props Prod.* **2022**, *189*, 115831. [CrossRef]
4. Krutov, S.M.; Voznyakovskii, A.P.; Gordin, A.A.; Savkin, D.I.; Shugalei, L.V. Environmental Problems of Wood Biomass Processing. Waste Processing Lignin. *Russ. J. Gen. Chem.* **2015**, *85*, 2898–2907. [CrossRef]
5. Wang, H.; Pu, Y.; Ragauskas, A.; Yang, B. From lignin to valuable products–strategies, challenges, and prospects. *Bioresour. Technol.* **2019**, *271*, 449–461. [CrossRef]
6. Tsvetkova, M.V.; Salganskii, E.A. Lignin: Applications and Ways of Utilization (Review). *Russ. J. Appl. Chem.* **2018**, *91*, 1129–1136. [CrossRef]
7. Voznyakovskii, A.P.; Savkin, D.I.; Kalinin, A.V.; Shugalei, I.V.; Krutov, S.M.; Mazur, A.S. Self-Propagating High-Temperature Synthesis as a Promising Method for the Utilization of Technical Lignins. *Russ. J. Gen. Chem.* **2016**, *86*, 3008–3011. [CrossRef]
8. *ISO/TS 80004-13:2017*; Nanotechnologies—Vocabulary—Part 13: Graphene and Related Two-Dimensional (2D) Materials. International Organization for Standardization: Geneva, Switzerland, 2017. Available online: https://www.iso.org/obp/ui/#iso:std:iso:ts:80004:-13:ed-1:v1:en (accessed on 8 January 2023).
9. Dolgoborodov, A.Y.; Streletskii, A.N.; Makhov, M.N.; Teselkin, V.A.; Guseinov, S.L.; Storozhenko, P.A.; Fortov, V.E. Promising Energetic Materials Composed of Nanosilicon and Solid Oxidizers. *Russ. J. Phys. Chem. B* **2012**, *6*, 523–530. [CrossRef]
10. Zegrya, G.G.; Savenkov, G.G.; Zegrya, A.G.; Bragin, V.A.; Os'kin, I.A.; Poberezhnaya, U.M. Laser Initiation of Energy-Saturated Composites Based on Nanoporous Silicon. *Tech. Phys.* **2020**, *65*, 1636–1642. [CrossRef]
11. Dolgoborodov, A.Y.; Kirilenko, V.G.; Brazhnikov, M.A.; Grishin, L.I.; Kuskov, M.L.; Valyano, G.E. Ignition of nanothermites by a laser diode pulse. *Def. Technol.* **2022**, *18*, 194–204. [CrossRef]

12. Collard, D.N.; Uhlenhake, K.E.; Örnek, M.; Rhoads, J.F.; Son, S.F. Photoflash and laser ignition of Al/PVDF films and additively manufactured igniters for solid propellant. *Combust. Flame* **2022**, *244*, 112252–112262. [CrossRef]
13. Sterletskii, A.N.; Dolgobrodov, A.Y.; Kolbanev, I.V.; Makhov, M.N.; Lomaeva, S.F.; Borunova, A.B.; Fortov, V.E. Structure of Mechanically Activated High-EnergyAl + Polytetrafluoroethylene Nanocomposites. *Colloid J.* **2009**, *71*, 852–860. [CrossRef]
14. Voznyakovskii, A.; Vozniakovskii, A.; Kidalov, S. New Way of Synthesis of Few-Layer Graphene Nanosheets by the Self Propagating High-Temperature Synthesis Method from Biopolymers. *Nanomaterials* **2022**, *12*, 657. [CrossRef]
15. Voznyakovskii, A.; Neverovskaya, A.; Vozniakovskii, A.; Kidalov, S. A Quantitative Chemical Method for Determining the Surface Concentration of Stone–Wales Defects for 1D and 2D Carbon Nanomaterials. *Nanomaterials* **2022**, *12*, 883. [CrossRef]
16. Patterson, A.L. The Scherrer Formula for X-Ray Particle Size Determination. *Phys. Rev.* **1939**, *56*, 978–982. [CrossRef]
17. Johra, F.T.; Lee, J.W.; Jung, W.G. Facile and safe graphene preparation on solution based platform. *J. Ind. Eng. Chem.* **2014**, *20*, 2883–2887. [CrossRef]
18. Li, C.; Zhang, X.; Wang, K.; Sun, X.; Liu, G.; Li, J.; Ma, Y. Scalable self-propagating high-temperature synthesis of graphene for supercapacitors with superior power density and cyclic stability. *Adv. Mater.* **2017**, *29*, 1604690. [CrossRef]
19. Ji, Q.; Wang, B.; Zheng, Y.; Zeng, F.; Lu, B. Field emission performance of bulk graphene. *Diam. Relat. Mater.* **2022**, *124*, 108940. [CrossRef]
20. Mao, L.F. Thermionic emission current in graphene-based electronic devices. *Appl. Phys. A* **2019**, *125*, 325. [CrossRef]
21. Rudi, S.G.; Faez, R.; Moravvej-Farshi, M.K. Effects of Stone-Wales defect on the electronic and transport properties of bilayer armchair graphene nanoribbons. *Superlattices Microstruct.* **2016**, *100*, 739–748. [CrossRef]
22. Voznyakovskii, A.P.; Fursei, G.; Vozniakovskii, A.A.; Polyakov, M.; Neverovskaya, A.; Zakirov, I. Low-threshold field electron emission from graphene nanostructures. *Fuller. Nanotub. Carbon Nanostructures* **2022**, *30*, 53–58. [CrossRef]
23. Fahd, A.; Dubois, C.; Chaouki, J.; Wen, J.Z. Nanothermites: Developments and Future Perspectives. In *Nano and Micro-Scale Energetic Materials: Propellants and Explosives*; Pang, W., DeLuca, L.T., Eds.; Part III Metal-based Pyrotechnic Nanocomposites. Chapter 8. Weinheim (FRG): Wiley-VCH 2023; Wiley: Hoboken, NJ, USA, 2023; Volume 1, pp. 219–251. [CrossRef]
24. Ilyushin, M.A.; Vedernikov, Y.N.; Voznyakovskii, A.P.; Shugalei, I.V.; Smirnov, A.V.; Kovalenko, A.I.; Butenko, V.G.; Kulagin, Y.A. 2D Graphene Structures Photoelectric Effect on Initiation of Cobalt (III) Perchlorate Complex Explosive Decomposition. *Ross. Khimicheskiy Zhurnal* **2021**, *65*, 24–29. (In Russian) [CrossRef]

Disclaimer/Publisher's Note: The statements, opinions and data contained in all publications are solely those of the individual author(s) and contributor(s) and not of MDPI and/or the editor(s). MDPI and/or the editor(s) disclaim responsibility for any injury to people or property resulting from any ideas, methods, instructions or products referred to in the content.